WPPFC-PR(18) 21032

C Porosnicu et al.

Dual-HiPIMS system as source of fusion related W-Al composite layers having deuterium inclusions

Preprint of Paper to be submitted for publication in
Surface and Coatings Technology

This work has been carried out within the framework of the EUROfusion Consortium and has received funding from the Euratom research and training programme 2014-2018 under grant agreement No 633053. The views and opinions expressed herein do not necessarily reflect those of the European Commission.

Dual-HiPIMS system as source of fusion related W-Al composite layers having deuterium inclusions

P. Dinca[a], V. Tiron[b], I. Mihaila[c], I.-L. Velicu[d], C. Porosnicu[a], B. Butoi[a],
A. Velea[e], F. Sava[e], E. Grigore[a], C. Costin[d], C.P. Lungu[a]

[a]*National Institute for Lasers, Plasma and Radiation Physics, Bucharest-077125, Romania*
[b]*Research Department, Faculty of Physics,AlexandruIoanCuza University, Iasi-700506, Romania*
[c]*Integrated Center of Environmental Science Studies in the North-Eastern Development Region (CERNESIM), AlexandruIoanCuza University of Iasi, Iasi-700506, Romania*
[d]*Faculty of Physics, AlexandruIoanCuza University, Iasi-700506, Romania*
[e]*National Institute of Material Physics, Bucharest-077125, Romania*

Corresponding Author: **Dr. Corneliu POROSNICU**
National Institute for Lasers, Plasma and Radiation Physics
Str. Atomistilor, nr. 409, Magurele - 077125, ROMANIA
Tel.: +40 214574468
Fax: +40 214574468
E-mail: corneliu.porosnicu@inflpr.ro

Abstract: Co-sputtering of tungsten-aluminum fusion relevant materials in a dual- High Power Impulse Magnetron Sputtering discharge, operated in different Ar-D_2 gas mixtures, was investigated by means of energy-resolving mass spectrometry. The average power on each target was varied between 5 and 100 W by adjusting the pulse repetition frequency and keeping constant the target voltage and pulse duration. Experimental results indicate that the total ion flux is strongly dependent on both sputtering gas composition and average power applied to the targets. During single HiPIMS operation with W target, the D^- ions are the most abundant species. The measured D^- ion flux shows an increase with the D_2 content in Ar-D_2 gas mixture and a linear increase with the power applied to the W target. In contrast, during dual-HiPIMS operation, a decrease of D^- ion flux was observed when the input power applied to the Al target was increased. The origin of different deuterium ion populations is also discussed. The structure and chemical composition of the W-Al coatings obtained in Ar-D_2 were investigated by means of X-ray diffraction and Glow Discharge Optical Emission Spectroscopy. The results indicate the presence of W cubic polycrystalline phase and that the deuterium retention increases with the tungsten atomic percentage in the deposited coatings. The intense and energetic bombardment of the growing film with D^- ions seems to be responsible for the large amount of D retained in the W-Al layers.

Keywords: Co-deposited mixed layer, Aluminium-tungsten, Deuterium retention, Ion energy distributions (IED); Gaseous inclusion in thin films.

1. Introduction

The dynamic development of civilization during the last 100 years is strongly linked to the availability of energy sources which are based mostly on fossil fuel used in both transportation and industry. The emerging clean renewable energies based on solar and wind power have a tremendous potential in covering the demand of domestic power consumption, but due to discontinuous exploitation, high costs, low yield and reliance on external meteorological factors. These energy resources are, however, somewhat unfit for use in industry. One promising power source for obtaining massive amounts of clean energy suitable for covering the ever-increasing demands is represented by nuclear fusion. This technology relies on the fusion of light hydrogen isotopes in magnetically confined plasma in a torus shaped device, known as tokamak. One of the serious concerns regarding the design of future nuclear fusion devices is represented by the erosion, migration and re-deposition processes of materials from plasma facing components under intense plasma wall interaction [1]. Materials eroded from the first wall and the divertor area can heavily contaminate the fusion plasma leading to energy absorption and plasma instabilities, such as edge localized modes, which can seriously damage the reactor. Another concern regards the in-vessel tritium (T) inventory which has an imposed limit of 700 g for International Thermonuclear Experimental Reactor (ITER) due to safety regulation [2]. The ITER vessel will be composed of beryllium (Be) and tungsten (W) [3], but due to safety regulations regarding the handling of T and Be, their use in experimental facilities is limited [4,5]. A similar material proposed first by Laurent Marot *et al* [6],in form of beryllium oxide and, possibly Be deuteride, is aluminum (Al), which can be used as a surrogate for Be in experimental studies, in many research facilities. Due to its proposal as a proxy for Be, Al coated surfaces were employed in a series of studies concerning the *in-situ* cleaning of ITER plasma diagnostic mirrors by means of pulsed lasers [7] and RF plasma cleaning with Arions [8].Other studies were focused on analyzing the sputtering yield, ablation properties and D retention in Al based coatings and samples. In an experiment performed with a PISCES B linear plasma accelerator by Krete*et al* [9], Al exhibits similar properties to Be in respect to morphological changes and sputtering yield under D plasma exposure,but different fuel retention mechanisms. Similar conclusions were drawn by Quiros *et al.* [10] who exposed Al samples in an electron-cyclotron resonance plasma reactor CASIMIR, at relevant D fluency of 10^{24} ions/m^2. An important domain were Al samples are required instead of Be, due to the high toxicity of the last in vapor form, is represented by Laser Induced Breakdown Spectroscopy (LIBS) measurements. Besides a limited number of LIBS experiments performed on Be

[11,12], most of ITER relevant studies were performed on Al based samples [13,14]. In Ref. [15],Suchonova *et al.* investigated and compared the ablation and fuel retention behaviors of W-Al and Be-W co-deposited samples. Their results indicate that the ablation rate and electron density are slightly higher for W-Al coating compared to Be-W, but the retention mechanisms are different.

In ITER, it is expected that the largest part of theT inventory to be retained in co-deposited layers, so it makes sense to obtain and study this type of layers using deuterium (D) as surrogate for T. A suitable method that can be used to obtain fusion relevant coatings with D gas inclusions is High Power Impulse Magnetron Sputtering (HiPIMS). As presented by Vladimir Kouznetsov *et al.* [16], HiPIMS can deliver to the magnetron cathode power densities of the order of tens of MW/m^2 per pulse. This can be significantly useful for obtaining coatings under similar conditions to those expected in a nuclear fusion reactor, where the power density loadings can reach up to 20 MW/m^2. Also, the high ionization yield obtained in a HiPIMS discharge helps to obtain ultra-dense coatings [17]. Usually, in a fusion reactor, ultra-dense coatings are expected to grow from sputtered material on the inner W divertor region. Another advantage is that HiPIMS discharge was already successfully implemented to obtain fusion relevant coatings containing W and Be [18,19].

In this contribution, the obtained results were presented in two distinct sections. The first section aims to characterize the W-Al co-sputtered ions in Ar-D_2 in a dual-HiPIMS discharge by means of mass spectrometry measurements. The ion flux composition is measured for different gas mixture compositions and input power delivered to the targets. The second section of this contribution is intended for the structural, morphological and chemical composition analysis of W-Al layers obtained in Ar-D_2 gas mixture. The influence of chemical composition on the deuterium retention was also investigated.

2. Materials and methods

Mass spectrometry measurements have been performed in order to characterize the W and Al co-sputtered ions in a dual-HiPIMS discharge in Ar-D_2 gas mixture. The ion flux composition at the substrate position was deduced from the time-averaged ion energy distribution functions (IEDFs) of both ionized sputtered metal and sputtering gas ions, which were measured using an energy-resolving mass spectrometer (EQP 1000, Hiden Analytical). Fig. 1 shows the schematic view of the experimental set-up which was provided with a dual-HiPIMS system and an ion detection system consisting of an energy-resolving mass

spectrometer. The dual-HiPIMS system consists of two identical magnetron cathodes (KurtJ. Lesker TORUS 2″), equipped with high purity (99.98%) W and Al targets and two identical HiPIMS power supplies. The HiPIMS power supplies were independently controlled by an external two channels TTL signal pulse generator, while the pulsed current and voltage waveforms were registered with an oscilloscope. The distance between the sputtering targets and the mass spectrometer nozzle was approximately 17 cm. W target was positioned in front of the mass spectrometer, facing directly the nozzle, while Al target was positioned sideways to the W target, at an angle of 45° from the spectrometer head axis (Fig. 1).

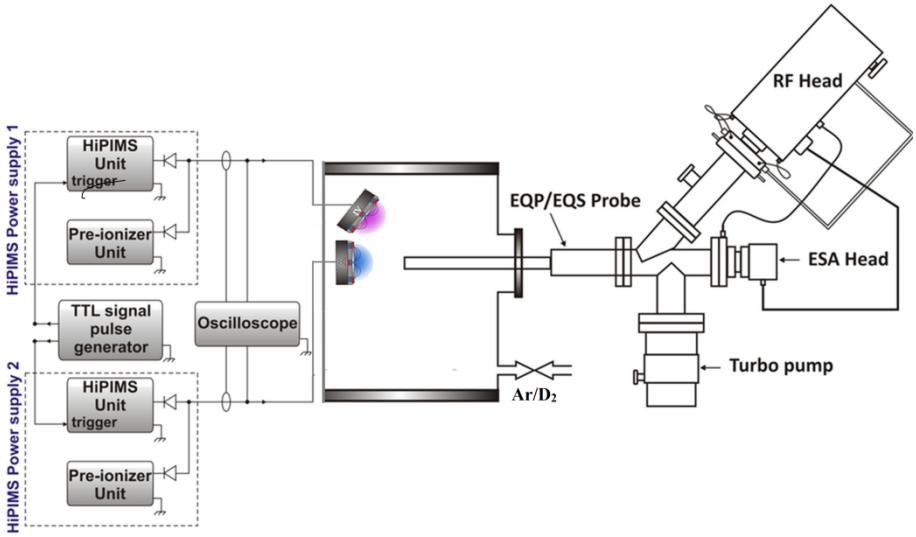

Fig. 1. Simplified scheme of the dual-HiPIMS system and mass spectrometer.

Previous experiments, not published yet, performed with a standard HiPIMS set-up, separately on W and Al targets, showed that using the same process parameters (gas pressure, gas composition, average discharge power, pulse duration, target-to-substrate distance), the Al^+ ion flux to the substrate is much higher as compared to W^+ ion flux. Therefore, in order to investigate plasma species, which lead to the growth of W-based layers with D gaseous inclusions, the average power on the W target was kept constant and set to 100 W, while the average power on the Al target was varied between 5 and 100 W, by independent manipulation of the pulsing repetition frequency. The electrical parameters of the HiPIMS power supply were: applied voltage of -1 kV, average power on W target of 100 W, pulse duration of 3 μs and gas pressure of 1 Pa with different gas mixtures of Ar-D_2.

In order to investigate the influence of the structure and chemical composition of W based thin films on D retention, three types of W-based thin films, with different Al

concentrations, were deposited on silicon (Si) substrates by dual High-Power Impulse Magnetron Sputtering (dual-HiPIMS) of W and Al targets in Ar-D_2 gas mixture, by adjusting the input power on each target. The geometry of the deposition set-up was similar to that presented in Fig. 1, with the mention that the substrates were placed closer to both sputtering targets than in the case of mass spectroscopy measurements. On both targets were applied high-voltage pulses with an amplitude of -1 kV and duration of 5 μs. The D_2 to Ar-D_2 mass flow ratio was set to 50%, while the total gas pressure was kept constant at 1 Pa. The Si substrates were placed at 10 cm from each target surface and, during the deposition process, they were electrically grounded and unintentionally heated. For the sake of the simplicity, the obtained samples were named S1, S2 and S3, corresponding to the following deposition conditions and chemical composition:

- S1: W-Al (W: 80 at. % - Al: 20 at. %);
- S2: W-Al (W: 90 at. % - Al: 10 at. %);
- S3: W-Al with gradient of Al content.

The chemical composition of the samples S1 and S2 was estimated based on the deposition rate measurements (by Quartz Crystal Microbalance) performed individually for each sputtered target, prior to the W-Al co-sputtering process. The sample S3, with Al gradient content, was obtained by gradually increasing the input power on the Al target and decreasing the input power on the W target.

A FEI Co., model Inspect S, scanning microscope was used to acquired surface images for the W-Al layers co-deposited in Ar-D_2 gas mixture. This set of images was taken at a working pressure of 1.5×10^{-2} Pa, distance of 14.9 mm, with 20 kV acceleration voltage and a magnification of 10000×. The second set of images was required for thickness measurements. The samples deposited on Si substrate were fractured into smaller pieces and cross-section measurements were performed in multiple regions, along the fracture line, to determine an average thickness of the layers. These measurements were performed at a base pressure of 1.56×10^{-2} Pa, distance of 11.9 mm, with 20kV acceleration voltage and 20000× magnification.

The structural analysis of W-Al layers deposited in Ar-D_2 was performed by means of grazing incidence X-ray diffraction (GIXRD). The measurements were conducted using a Bruker D8 Advance–diffractometer provided with CuK_α target tube (λ = 0.154178 nm), scintillation counter and Göbell mirror in a grazing incident configuration (θ_i = 3°). The patterns have been recorded with an angular step of 0.04° (2θ), and a counting time per step

of 2 s. In order to avoid systematic errors in the X-ray data, before each GIXRD measurement, sample alignment and diffractometer adjustments were conducted.

Glow discharge optical emission spectroscopy (GDOES) measurements of W-Al layers obtained in Ar-D_2 gas mixture were performed with a GDA 750 HR instrument from *Spectruma*. The instrument is provided with photomultiplier tubes used to measure up to 29 fixed analytical elemental channels and capable of delivering high spatial resolution (nanometer size), analytical precision and flexibility. Therefore, these characteristics proved highly reliable in obtaining depth profiles to accurately determine the chemical composition of layers.

3. **Results and discussion**

3.1.Mass spectrometry characterization of W-Al co-sputtered in Ar-D_2 gas mixture

The time-averaged IEDFs of Al^+, W^+, W^{++} co-sputtered species and Ar^+, Ar^{++}, D^+, D^-, D_2^+ and D_3^+ sputtering gas species were recorded during single HiPIMS discharge in order to investigate the influence of the average power delivered to the target and the influence of the gas mixture on the ion flux composition. The sputtering gas composition was changed by adjusting the D_2 to Ar mass flow ratio to 0/100, 25/75, 50/50 and 75/25. The processing parameters are the ones mentioned in **Materials and Methods** section of this paper. It is worth mentioning that, depending on the gas composition, the peak current varies between 18 and 25 A, in the case of HiPIMS of W target, and between 13 and 25 A, in the case of HiPIMS of Al target. The higher peak current values correspond to the case when the discharge works only in Ar gas, while the lower values correspond to the case in which D_2 to Ar mass flow ratio was 75/25..For each ion species, the flux was calculated as the integral of the IEDF. The total ion flux composition (expressed as percentage) was deduced by diving each ion specie flux to the total ion flux.

A detailed study of the W ion energy distributions in high-power pulsed magnetron sputtering discharges was carried out in our recent work [20]. In this paper, our attention has been focused on deuterium ion energy distribution functions. Due to high electron density in HiPIMS Ar-D_2 plasma, it is expected the dissociation of D_2 molecular gas to be enhanced, which will lead to multiple reaction products as D, D^+, D^-, D_3, D_3^+. The presence of multiple deuterium ion species (both positive and negative) has been confirmed by mass spectrometry measurements (Fig.2).The results are illustrated in Fig.2and they were obtained when only the

W target was sputtered in single HiPIMS mode, at an average power of 100 W. Mass spectrometry measurements indicated the lack of compound ion species such as WD^+ in HiPIMS plasma.

The origin of deuterium positive ions D^+, D_2^+ and D_3^+ is near the target, in the ionization region, where the following reactions take place [21]:

- $D_2 + e^- \rightarrow D_2^+ + 2e^-$
- $D_2 + e^- \rightarrow D^- + D$
- $D_2^+ + D_2 \rightarrow D_3^+ + D$
- $D_2^+ + D \rightarrow D_3^+$
- $D + e^- \rightarrow D^+ + 2e^-$.

The time-averaged ion energy distributions ofD_2^+ and D_3^+ molecules, which are produced through the reactions mentioned above, show only a peak at low ion energy of about 1 eV. The low energy peak originates from thermal molecular ions which are produced in the plasma volume and are accelerated towards the instrument through the plasma sheath formed in front of the extraction orifice. The maximum detected energy for these molecular ion species is only 10 eV. The time-averaged ion energy distribution functions are more different for D^+ and D^- ions:they have a maximum around 1 eV and a very high energy tail, which extends up to 500 eV. Negative ions aremainly produced in the ionization region of the HiPIMS plasma via dissociative electron attachment($D_2 + e^- \rightarrow D^- + D$), being thenrepelled by the highly negative potential of the target. This statement is supported by previous experimental results, which shown that during magnetron sputtering,the negative ions (such as O^-) that are generated in front of the target surface are accelerated towards the substrate by the full negative target potential [22,23].Mráz*et al.*suggested that the high energy gas ions may be generated at the cathode surface through desorption of negative ions or neutral atoms followed by electron attachment and subsequent acceleration over the cathode fall [24]. In our case, due to relative high gas pressure (1 Pa) and lighter gas ions, the maximum detected energy is lower than energy gained by the negative ions in the full negative target potential (up to 1 kV). During their transport towards the mass spectrometer, deuterium ions lose a part of kinetic energy due to the collisions process. In addition, depending on the place where they are produced, the negative D^- ion may experience only a fraction of the full target potential.The energy distribution function shows low (energies up to 10 eV), medium, and high energy (energies higher than 50 eV) D^- ion populations.

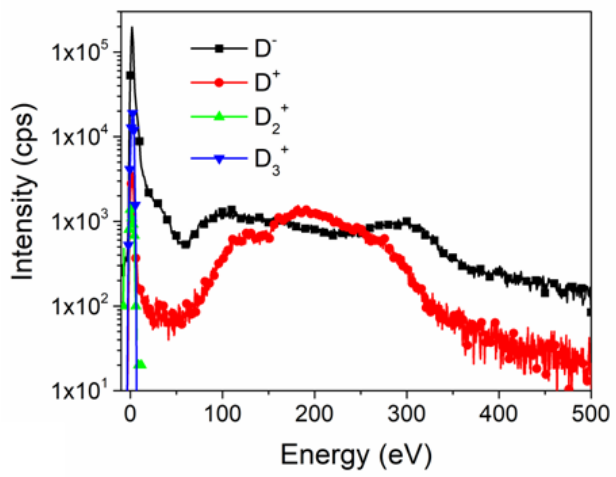

Fig. 2. IEDFs of deuterium ion species during single HiPIMS mode operation with W target in Ar-D_2 gas mixtures. Average discharge power was 100 W, whileD_2/(D_2+Ar) mass flow ratio was 50%.

The origin of the high energy D^+ ion populations (Fig. 2) may be as follows: a fraction of the D^- energetic ions may be neutralized by collisions with plasma species and then ionized in their way towards the mass spectrometer leading to the occurrence of D^+ energetic ions.

The ion flux composition during dual-HiPIMS operation with W and Al targets in Ar-D_2 gas mixture is shown in Fig.3(a), (b) and (c). Because D_2^+, D_3^+, Ar^{++}, Ar^+ and W^{++} ion fluxes are very low, we chose to plot only the D^-, D^+, Al^+ and W^+ species. For the same value of the input power (total average power applied on Al and W targets), as the Ar sputtering gas is replaced by D_2, the ion flux composition changes due to the increase of deuterium (D^+ and D^-) ion flux and the decrease of W ion flux.

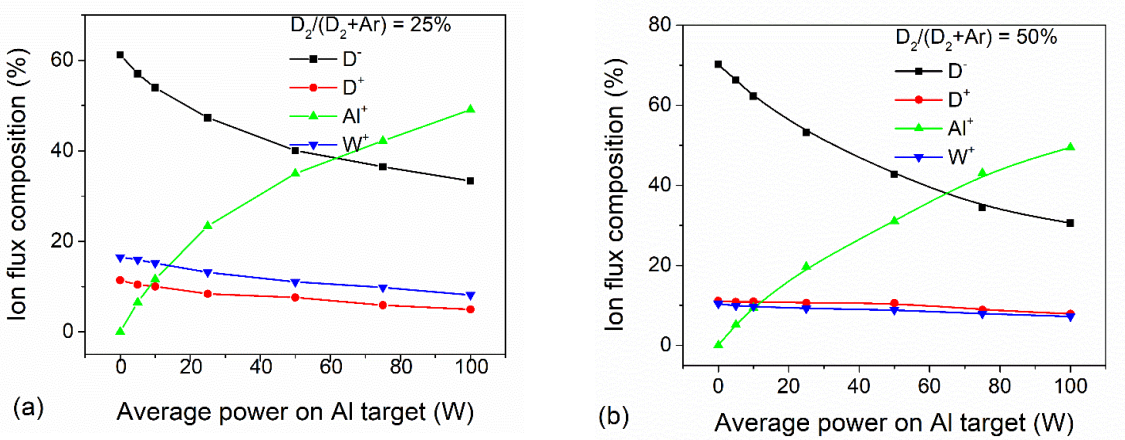

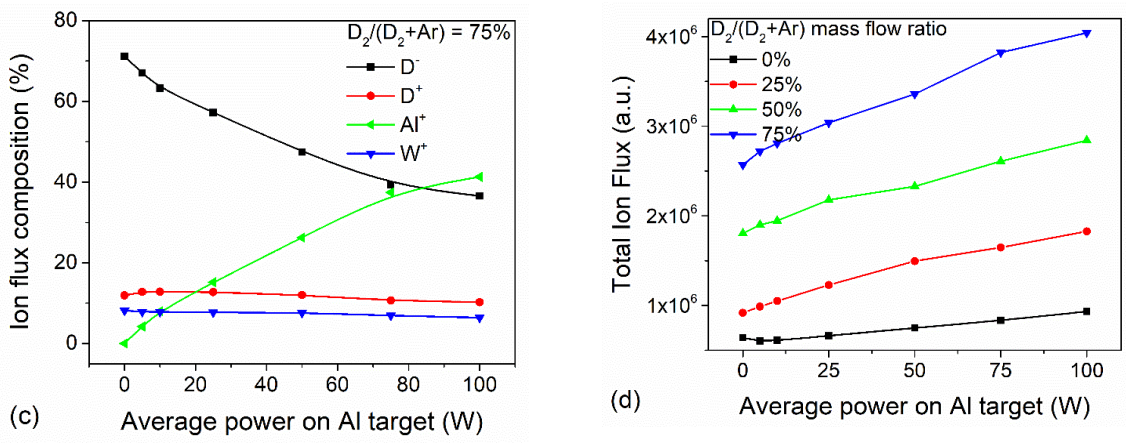

Fig. 3. Ion flux composition during dual-HiPIMS operation with W and Al targets in Ar-D_2 gas mixture, at different values of the average power applied on the Al target and different sputtering gas compositions (a-c) and the total ion flux (d). The average power on the W target was 100 W.

The influence of the average power on the Al target, as well as the influence of the gas mixture on the ion flux composition, is shown in Figure 3(d). The total ion flux increaseswiththe increase of the input power and/or the $D_2/(D_2+Ar)$ mass flow ratio. This behavior may be related to the higher electron density and temperature which facilitate the occurrence of both electron impact dissociative attachment reactions (generation of D^- negative ions) and ionization processes (generation of D^+, Al^+ and W^+ ions). Both the average power applied on the Al target and the sputtering gas compositions have a strong influence on the total ion flux.

3.2.Mass spectrometry investigation on D^- ions

This task was developed because the measurements on the ion energy distribution function (IEDF), during co-sputtering of W and Al targets in dual-HiPIMS mode, in Ar-D_2 gas mixture, have shown the presence of a large fraction of D^- ions in the total ion flux. Due to their abundance, high kinetic energy and associated effects on growing films, a particular attention was paid to the influence of processing parameters on D^- ions flux. The production of D^- negative ions occurs through the dissociative attachment reactions from highly vibrationally excited molecules $D_2(v)$ [21]:

$$D_2(v) + e^-_{slow} \rightarrow D^- + D$$

where $D_2(v)$ are produced through the following reactions:

- $D_2(v=0) + e^-_{fast} \rightarrow D_2^* + e^-_{fast}$

- $D_2^* \rightarrow D_2(v) + h\nu$.

This statement is sustained by the optical emission spectroscopy measurements (not shown here) which indicate the presence of D_α and D_β neutral spectral lines and Fulcher α-band (attributed to highly vibrationally excited D_2 molecules) in the global emission spectra of HiPIMS Ar-D_2 plasma.Consequently, the production of D_2 occurs through electron impact dissociation from highly vibrationally excited molecules $D_2(v)$ which, in their turn, are generated by fast electron collisions. It is expected that an increase in the input power and/or the $D_2/(D_2+Ar)$ mass flow ratio to lead to a higher electron density and temperature which, in turn, facilitates the occurrence of electron impact dissociative attachment reactions and generation of more D^- negative ions.

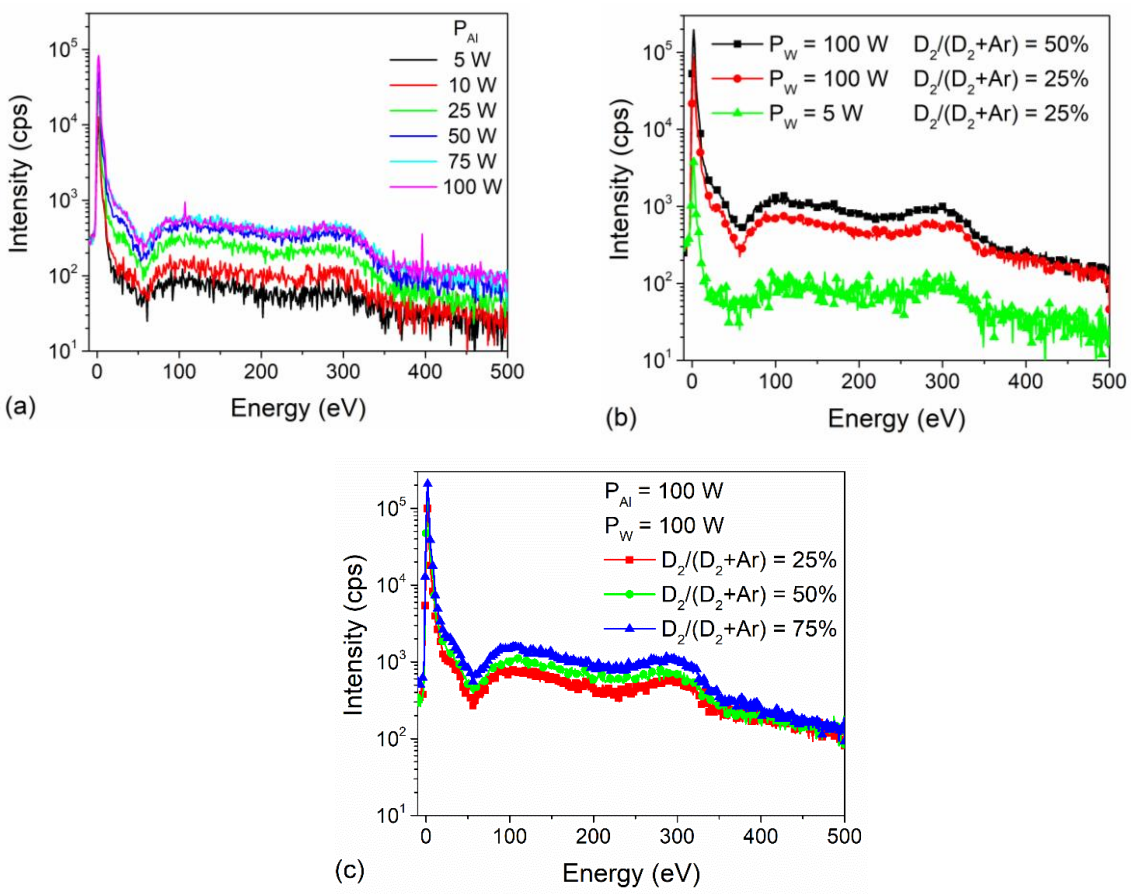

Fig. 4.EDFs of D^- ions for different discharge conditions: (a) standard HiPIMS mode operated with Al target at different input powers, with $D_2/(D_2+Ar)$ = 50%; (b) standard HiPIMS mode operated with W target at different input powers and different Ar-D_2 gas mixtures; (c) dual-HiPIMS operation with W and Al targets in different Ar-D_2 gas mixtures (both targets operate at 100 W).

Figs.4(a), (b) and (c) show the time-averaged IEDFs of D^- ions for different discharge conditions: (a) standard HiPIMS mode operated with Al target at different input powers, with $D_2/(D_2+Ar)$ = 50%; (b) standard HiPIMS mode operated with W target at different input powers and different Ar-D_2 gas mixtures and (c) dual-HiPIMS operation with W and Al targets in different Ar-D_2 gas mixtures (both targets operate at 100 W). The energy distribution functions of D^- ions show a maximum around 1 eV and a very high energy tail which extends towards 500 eV. The high-energy tail structure is related to the D^- ions which are produced in the ionization region of the HiPIMS plasma through the dissociative attachment from highly vibrationally excited D_2 molecules and then they are repelled by the highly negative potential of the target.

From Fig. 4(a) it can be noticed that an increase of the input power leads to an increase of both low and high energy part of the IEDF of D^-. The D^- ion flux, calculated as the integral of the IEDF, increases with the input power on the Al target and tends to saturate for the average power higher than 50 W. Fig.4(b) shows that an increase of the input power and/or the $D_2/(D_2+Ar)$ mass flow ratio leads to an increase of both low and high energy part of the IEDF of D^-. During dual-HiPIMS operation with the input power on each target set to 100 W, an increase of the $D_2/(D_2+Ar)$ mass flow ratio also leads to an increase of the entire IEDF of D^- (Fig.4(c)). Comparing Figs.4(a) and 4(b), for the same average power applied on both W and Al targets (100 W) and for the same ratio $D_2/(D_2+Ar)$ = 50%, the entire IEDF of D^- ions is higher when the discharge is operated with W target. When the discharge is operated in dual mode, with both targets powered at 100 W (Fig.4(c)), a small change of the IEDF of $D^-$is noticed with respect to the case of the discharge operated in standard HiPIMS mode, with W target (Fig.4(b)).

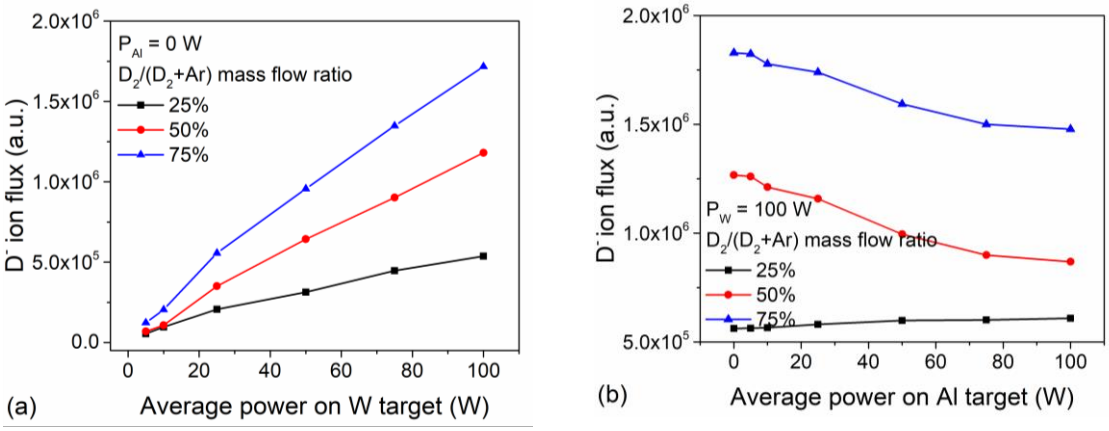

Fig.5.(a) D^- ion flux measured in standard HiPIMS mode with W target, for different Ar-D_2 gas mixtures, versus the input power; (b) D^- ion flux measured in dual-HiPIMS mode with W and Al targets, at different input powers on the Al target and for different Ar-D_2 gas mixtures.

Fig.5(a) shows the D^- ion flux versus the average power measured during standard HiPIMS mode operation with W target, in different Ar-D_2 gas mixtures. Fig.5(b) shows the dependence of D^- ion flux on average power delivered at Al target, but for the dual-HiPIMS operation, with the average power on theW target set to a constant value of 100 W. During standard HiPIMS of W target (power on Al is turned off), the D^- ion flux linearly increases with the input power on the W target and with the increase of $D_2/(D_2+Ar)$ mass flow ratio. This behavior may be related to the enhanced electron density and temperature which facilitate the occurrence of electron impact dissociative attachment reactions, leading to an increased population of D^- negative ions in the HiPIMS discharge. During dual-HiPIMS operation, at high $D_2/(D_2+Ar)$ mass flow ratio (50 and 75%), the D^- ion flux tends to slowly decrease as the average power on Al target increases due to the change of the plasma composition in front of the target, the working gas being replaced by sputtered Al atoms.

3.3.Morphological, structural and chemical composition of W-Al co-deposited thin films in Ar-D_2 gas mixture

Cross-sectional SEM image of the sample S3 (fracture cross-section) is shown in Fig.6. According to this image, the coating appears very dense, showing a homogeneous microstructure, without indications of columnar growth, which is a sign of a high film packing. The main mechanism responsible for the film densification is the intense and energetic bombardment of the growing film with heavy particles, both W and Ar ions. Previous studies have shown that during HiPIMS operation with short pulses, the fraction of the ionized W in the total flux is up to 50% and the energetic tail of W ions IEDF extends towards 100 eV [20].

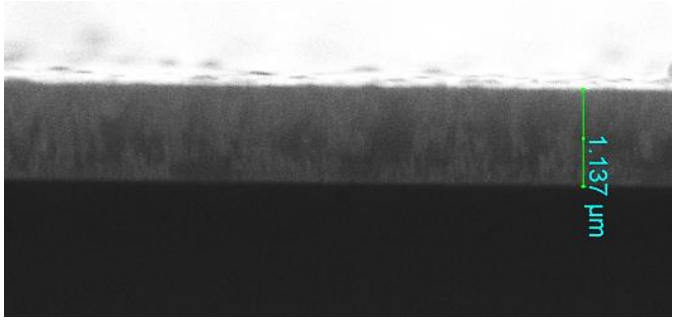

Fig.6. SEM cross-section image of W-Al thin film with Al concentration gradient deposited on Si substrate.

The GIXRD studies were carried out in order to identify the crystallinity and various phases present in the W based thin films. In the XRD pattern displayed in Fig.7, three peaks corresponding to the reflection of the X-rays on the atomic planes (200), (210) and (211) of the W cubic structure were identified. The XRD pattern revealed that the W-Al (W: 80 at.% - Al: 20 at.%) thin film is polycrystalline and preferentially oriented along (210) plane, while the W-Al (W: 90 at.% - Al: 10 at.%) thin film is crystalline, being oriented along (210) plane. The W-Al thin film with Al content gradient seems to be amorphous.

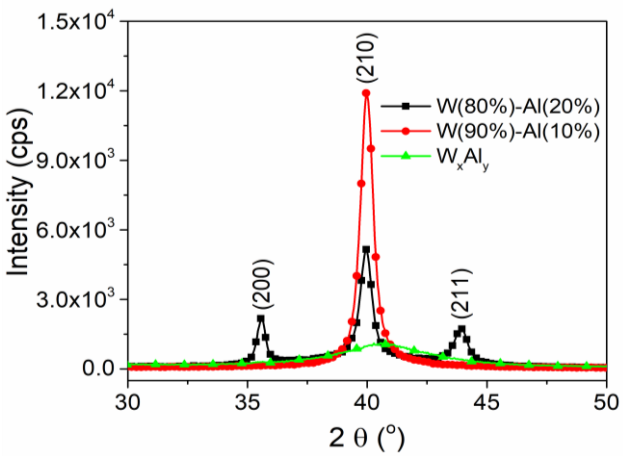

Fig. 7. GIXRD patterns of W-Al thin films deposited on Si substrates.

The W-Al thin film with Al content gradient is amorphous. Average crystallite size for the W phase is 9.9 nm (estimated from the (210) peak), while for the W_xAl_y layer is 9.4 nm (computed using the (110) peak).

The GDOES profiles (Figs.8 and 9) indicate the presence of a different amount of deuterium in the W-Al thin films.

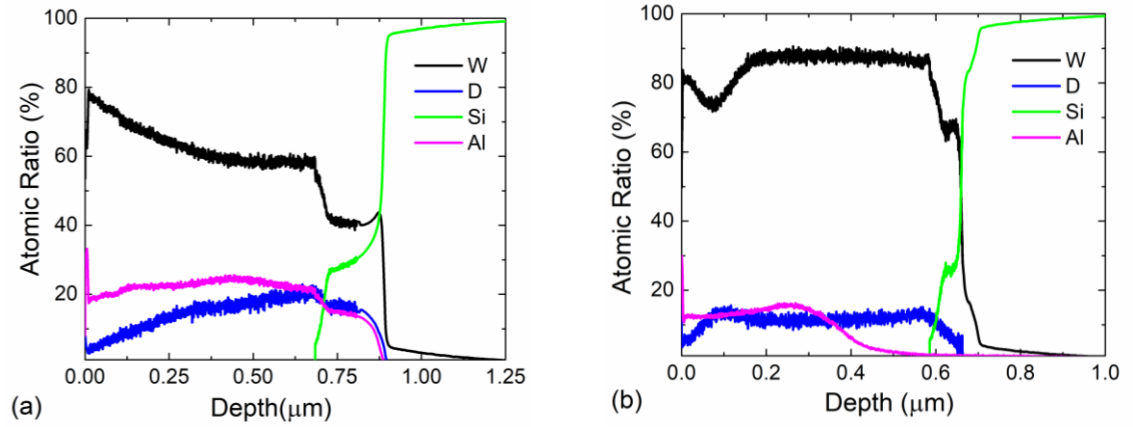

Fig. 8. GDOES depth profiles for the W(80%)-Al(20%) (a) and W(90%)-Al(10%) (b) thin films deposited on Si substrates.

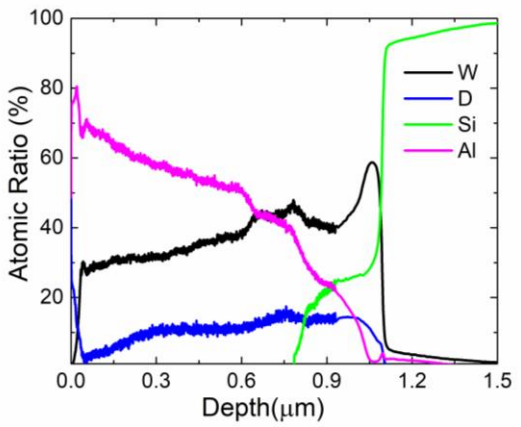

Fig.9. GDOES depth profiles for the W-Al thin film with gradient of Al content.

The largest amount of D was found in the sample S1 (Fig.8(a)), the maximum concentration was observed in the vicinity of the substrate (at the early stage of the deposition) being 21 at.%, This profile can be the result of the changes occurred on deposition conditions such as an increase of substrate temperature during deposition process that might trigger the D diffusion, but this hypothesis should be checked. The GDOES profiles of the sample S2 (Fig.8b) indicate the presence of less aluminum near the Si substrate due to the surface contamination of the Al target with residual oxygen (since the average power on the Al target was lower with respect to the case of S1 deposition). Depth profiles behavior indicates that the D retention in the W-Al layer is mainly related to the W in-depth concentration and less dependent on the Al one. GDOES depth profiles for the W-Al thin film with Al content gradient (Fig.9) show that increasing the Al concentration in the W-Al film, the amount of D tends to decrease. The depth profile of D has almost the same evolution as W in-depth profile. This behavior may be related to the fact that the D embedded in the layer comes mainly from the discharge developed in front of the W target, most probably as D^- ions.

4. Conclusions

Mass spectrometry measurements have been performed during dual High-Power Impulse Magnetron Sputtering (dual-HiPIMS) to characterize the W and Al co-sputtered material in D_2-Ar plasma. The ion flux composition at the substrate position was deduced from the time-averaged ion energy distribution functions (IEDFs) of both ionized sputtered metal and sputtering gas ions. The total ion flux and its composition strongly depend on the target material, gas mixture composition and the input power delivered to each target. The total ion

flux increases with the increase of the electrical power applied to each target and with the increase of the lighter gas (D_2) fraction in the sputtering gas mixture. During W and Al co-sputtering process in Ar-D_2 gas mixture, for an average power applied to the Al target lower than 60 W, the ion flux at the substrate position is dominated by D^- negative ions, while for an input power on Al target higher than 60 W, the ion flux at the substrate position is dominated by Al^+ ions.The energy distribution functions of D^- negative ions show a maximum around 1 eV and a very high energy tail which extends towards 500 eV. During standard HiPIMS operation, the D^- ion flux linearly increases with the average power on the W target and with the increase of $D_2/(D_2+Ar)$ mass flow ratio. During dual-HiPIMS operation, at high $D_2/(D_2+Ar)$ mass flow ratio (50 and 75%), the D^- ion flux tends to decrease as the input power on the Al target increases. GDOES profiles indicate the presence of a large amount of deuterium in the W-Al layers, with a maximum value in the case of W(80%)-Al(20%) films. Depth profiles indicate that the D distribution in the W-Al layers is related to the W in-depth concentration and not to the Al one. Experimental results show that the main mechanism responsible for the D retention in the W-Al layers is the intense and energetic bombardment of the growing film with D^- ions. Experimental results indicate that the HiPIMS discharge is a suitable model systemto simulate the plasma-wall interaction in fusion devices and also an efficient source for negative ion production.

Acknowledgements

This work has been carried out within the framework of the EUROfusion Consortium and has received funding from the Euratom research and training programme 2014–2018 under grant agreement No 633053. The activity was performed in the scope of the WP PFC programme. The views and opinions expressed herein do not necessarily reflect those of the European Commission.

References

[1] G. Federici, R.A. Anderl, P. Andrew, J.N. Brooks, R.A. Causey, J.P. Coad, D. Cowgill, R.P. Doerner, A.A. Haasz, G. Janeschitz, W. Jacob, G.R. Longhurst, R. Nygren, A. Peacock, M.A. Pick, V. Philipps, J. Roth, C.H. Skinner, W.R. Wampler, In-vessel tritium retention and removal in ITER, J. Nucl. Mater. 266 (1999) 14–29.

[2] K. Sugiyama, C. Porosnicu, W. Jacob, J. Roth, Th. Dürbeck, I. Jepu, C.P. Lungu, Study of deuterium retention in/release from ITER-relevant Be-containing mixed material layers implanted at elevated temperatures, J. Nucl. Mater. 438 (2013) S1113-S1116.

[3] G. Federici, P. Andrew, P. Barabaschi, J. Brooks, R. Doerner, A. Geier, A. Herrmann, G. Janeschitz, K. Krieger, A. Kukushkin, A. Loarte, R. Neu, G. Saibene, M. Shimada, G. Strohmayer, M. Sugihara, Key ITER plasma edge and plasma-material interaction issues, in: J. Nucl. Mater., 2003: pp. 11–22.

[4] M. Wisse, L. Marot, B. Eren, R. Steiner, D. Mathys, E. Meyer, Laser damage thresholds of ITER mirror materials and first results on in situ laser cleaning of stainless steel mirrors, Fusion Eng. Des. 88 (2013) 388–399.

[5] B. Eren, L. Marot, M. Wisse, D. Mathys, M. Joanny, J.M. Travère, R. Steiner, E. Meyer, In situ evaluation of the reflectivity of molybdenum and rhodium coatings in an ITER-like mixed environment, J. Nucl. Mater. 438 (2013).

[6] L. Marot, C. Linsmeier, B. Eren, L. Moser, R. Steiner, E. Meyer, Can aluminium or magnesium be a surrogate for beryllium: A critical investigation of their chemistry, in: Fusion Eng. Des., 2013: pp. 1718–1721.

[7] M. Wisse, L. Marot, R. Steiner, D. Mathys, A. Stumpp, M. Joanny, J. M. TravÈegrave;re & E. Meyer Picosecond and Nanosecond Laser Ablation of Mixed Tungsten/Aluminum Films, FUSION SCI TECHNOL 66 issue 2 (2017), 308-314

[8] L. Moser, R. Steiner, F. Leipold, R. Reichle, L. Marot, E. Meyer, Plasma cleaning of ITER First Mirrors in magnetic field, J. Nucl. Mater. 463 (2015) 940–943.

[9] A. Kreter, T. Dittmar, D. Nishijima, R.P. Doerner, M.J. Baldwin, K. Schmid, Erosion, formation of deposited layers and fuel retention for beryllium under the influence of plasma impurities, in: Phys. Scr., 2014.

[10] C. Quirós, J. Mougenot, G. Lombardi, M. Redolfi, O. Brinza, Y. Charles, A. Michau, K. Hassouni, Blister formation and hydrogen retention in aluminium and beryllium: A modeling and experimental approach, Nucl. Mater. Energy. 12 (2017) 1178–1183.

[11] J. Karhunen, A. Hakola, J. Likonen, A. Lissovski, M. Laan, P. Paris, Applicability of

LIBS for in situ monitoring of deposition and retention on the ITER-like wall of JET - Comparison to SIMS, J. Nucl. Mater. 463 (2015) 931–935.

[12] J. Karhunen, A. Hakola, J. Likonen, A. Lissovski, P. Paris, M. Laan, K. Piip, C. Porosnicu, C.P. Lungu, K. Sugiyama, Development of laser-induced breakdown spectroscopy for analyzing deposited layers in ITER, in: Phys. Scr., 2014.

[13] R. Hai, N. Farid, D. Zhao, L. Zhang, J. Liu, H. Ding, J. Wu, G.N. Luo, Laser-induced breakdown spectroscopic characterization of impurity deposition on the first wall of a magnetic confined fusion device: Experimental Advanced Superconducting Tokamak, Spectrochim. Acta - Part B At. Spectrosc. 87 (2013) 147–152.

[14] D. Zhao, N. Farid, R. Hai, D. Wu, H. Ding, Diagnostics of first wall materials in a magnetically confined fusion device by polarization-resolved laser-induced breakdown spectroscopy, Plasma Sci. Technol. 16 (2014) 149–154.

[15] M. Suchoňová, P. Veis, J. Karhunen, P. Paris, M. Pribula, K. Piip, M. Laan, C. Porosnicu, C. Lungu, A. Hakola, Determination of deuterium depth profiles in fusion-relevant wall materials by nanosecond LIBS, Nucl. Mater. Energy. 12 (2017) 611–616.

[16] V. Kouznetsov, K. MacÁk, J.M. Schneider, U. Helmersson, I. Petrov, A novel pulsed magnetron sputter technique utilizing very high target power densities, Surf. Coatings Technol. 122 (1999) 290–293.

[17] M. Samuelsson, D. Lundin, J. Jensen, M.A. Raadu, J.T. Gudmundsson, U. Helmersson, On the film density using high power impulse magnetron sputtering, Surf. Coatings Technol. 205 (2010) 591–596.

[18] V. Tiron, I. Velicu, C. Porosnicu, I. Burducea, P. Dinca, P. Malinský, Tungsten nitride coatings obtained by HiPIMS as plasma facing materials for fusion applications, Appl. Surf. Sci. 416 (2017) 878–884.

[19] P. Dinca, C. Porosnicu, B. Butoi, I. Jepu, V. Tiron, O.G. Pompilian, I. Burducea, C.P. Lungu, I.-L. Velicu, Beryllium-tungsten study on mixed layers obtained by m-HiPIMS/DCMS techniques in a deuterium and nitrogen reactive gas mixture, Surf. Coat. Technol.321 (2017) 397-402

[20] I.L. Velicu, V. Tiron, C. Porosnicu, I. Burducea, N. Lupu, G. Stoian, G. Popa, D. Munteanu, Enhanced properties of tungsten thin films deposited with a novel HiPIMS approach, Appl. Surf. Sci. 424 (2017) 397–406.

[21] C. Gorse, M. Capitelli, Enhanced production of negative ions in low-pressure hydrogen and deuterium pulsed discharges: Theoretical calculations, Phys. Rev. A. 46 (1992) 2176–2177.

[22] K. Sarakinos, D. Music, S. Mráz, M. To Baben, K. Jiang, F. Nahif, A. Braun, C. Zilkens, S. Konstantinidis, F. Renaux, D. Cossement, F. Munnik, J.M. Schneider, On the phase formation of sputtered hafnium oxide and oxynitride films, J. Appl. Phys. 108 (2010).

[23] M. Bowes, P. Poolcharuansin, J.W. Bradley, Negative ion energy distributions in reactive HiPIMS, J. Phys. D. Appl. Phys. 46 (2013).

[24] S. Mráz, J.M. Schneider, Energy distribution of O- ions during reactive magnetron sputtering, Appl. Phys. Lett. 89 (2006) 89–91.